Structural Principles and Amorphouslike Thermal Conductivity of Na-Doped Si Clathrates

J. S. Tse, K. Uehara, R. Rousseau, A. Ker, and C. I. Ratcliffe
Steacie Institute for Molecular Sciences, National Research Council of Canada, Ottawa, Ontario, Canada K1A 0R6

M. A. White and G. MacKay
Department of Chemistry, Dalhousie University, Halifax, Nova Scotia, Canada B3H 4J3
(Received 20 January 2000)

The postulated low thermal conductivity and the possibility of altering the electronic conductivity of metal-doped clathrates with semiconducting host elements have stimulated great interest in exploring these compounds as promising thermoelectric materials. The electronic and thermal properties of the prototypical Na_xSi_{46} system are studied in detail here. It is shown that, despite the fact that the Na/Si clathrate is metallic, its thermal conductivity resembles that of an amorphous solid. A theoretical model is developed to rationalize the structural stability of the peculiar structural topology, and a general scheme for rational design of high efficiency thermoelectric materials is presented.

PACS numbers: 61.72.Tt, 66.70.+f, 71.20.–b, 72.15.Qm

The key characteristic for materials with high thermoelectric power is governed by the dimensionless quantity $ZT = TS^2\sigma/\kappa$, where S is the Seebeck coefficient, σ is the electrical conductivity, and κ is the thermal conductivity. The obvious approach is to design novel materials that behave electrically as semiconductors but thermally as amorphous solids. Several strategies have been employed to satisfy these criteria [1]. It is well known that doping of a crystalline solid with impurities that possess low frequency localized vibrations is an effective way to reduce the thermal conductivity [2–4]. Typical compounds which have been considered are analogs of Na-doped Si clathrates [5,6]. These Si clathrates exist in two structure types [7] and are very versatile materials whose properties can be altered via the manipulation of the concentration and nature of the dopant [8,9]. In spite of several calculations [10,11] on the electronic structure and vibrational properties [12,13] of Si clathrates, no information regarding the *origin* of the structural stability and the thermoelectric power is available. The objective of this investigation is to examine the fundamental principles that underlie these promising thermoelectric properties and to suggest systematic improvements based upon these findings.

The thermal conductivity of a crystalline solid can have a glasslike temperature dependence. This unusual behavior is well characterized for clathrate hydrates [14] which are nonstoichiometric porous inclusion compounds with water molecules forming the host framework in which guest atoms or molecules can be trapped. This anomalous behavior was attributed to resonant scattering of the acoustic phonons by the localized guest vibrations [14–16] and recently has been confirmed experimentally [17]. If a clathratelike semiconductor with trapped guests could be synthesized, it is anticipated that its thermal conductivity would possess this desirable property, and thus it would be a potentially highly efficient thermoelectric material [9]. To test these ideas for Na-doped Si clathrates the thermal diffusivity D of a sample with a nominal stoichiometry of structure I Na_8Si_{46} has been measured over the temperature range 80–200 K. Measurements were performed with a modulated heat flow device [18]. The measured thermal diffusivities were converted to thermal conductivities, κ, by the relationship $\kappa = DC$, where C is the heat capacity per unit volume, determined from the specific heat [19] and density [20]. The thermal conductivities are shown in Fig. 1. The relatively large absolute error ($\pm 30\%$) is due to the low thermal diffusivity and small sample volume. The experimental data, about 0.42 $W\,m^{-1}\,K^{-1}$ at 80 K, indicate that the thermal conductivity of Na-doped Si clathrate is significantly lower than crystalline Si in this temperature range. Within the limits of accuracy the measured thermal conductivity remains constant with temperature, or possibly decreases with decreasing temperature, and the profile resembles that of an amorphous solid. The observed behavior closely follows that for clathrate hydrates [14–16]. Furthermore, it was shown that the thermal conductivity in gas hydrates could be described by a modified Einstein oscillator model [15,20]. The calculated minimum thermal conductivity [21] for Na_8Si_{46} is

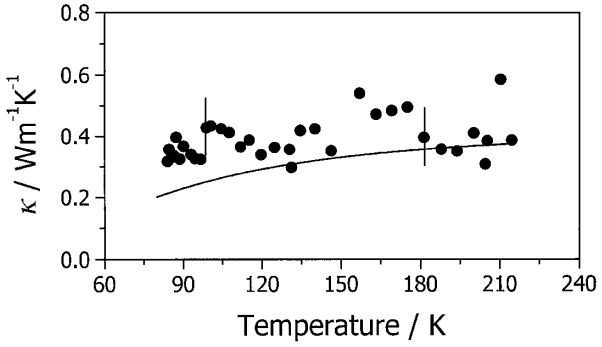

FIG. 1. Experimental (●) thermal conductivity, κ, for Na_8Si_{46}. The vertical bar indicates typical experimental uncertainty. The full line indicates the theoretical minimum thermal conductivity.

 0031-9007/00/85(1)/114(4)$15.00

shown in Fig. 1, and the experimental results indicate that thermal resistance is almost at its maximum efficiency. To effectively reduce the thermal conductivity, resonant phonon scattering must occur at the avoided crossing of the phonon branches where the localized guest vibrations have the same symmetry as the framework acoustic phonons [16]. In a recent measurement of the phonon density of states of Na_8Si_{46}, a sharp peak at 83 cm^{-1} was attributed to the localized vibration of the Na atom [22]. Moreover, tight-binding calculations predict that the maximum of the longitudinal acoustic branch of the empty framework is at 100 cm^{-1} [12,13]. Therefore, it appears that the necessary conditions for efficient phonon scattering have been satisfied.

Having examined the thermal behavior we now examine the electronic aspects of this problem. Electronic band structures obtained from full potential linearized augmented plane wave (FLAPW) calculations [23] are shown, respectively, in Figs. 2(a) and 2(b) for $Na_{24}Si_{136}$ and Na_8Si_{46} as well as the corresponding calculations on the hypothetical empty Si_{136} [Fig. 2(c)] and Si_{46} [Fig. 2(d)] frameworks. In both cases, the Na-Si clathrates and their Si analog provide very similar band structures *both* in the shape and relative dispersion of the bands. The electron density of states (DOS) and its projection onto the Na and Si (not shown) indicate that both structures are metallic and the majority of the electron density may be ascribed to Si. This indicates that the Na-Na and Na-Si interaction is predominantly ionic and that Na acts primarily as an electron donor [11]. A similar conclusion was reached in a rigid band study of K-doped Ge clathrate [24]. This result suggests that a *qualitative* analysis based upon the bands of the isolated Si framework may serve to understand the properties of Na-doped Si clathrates.

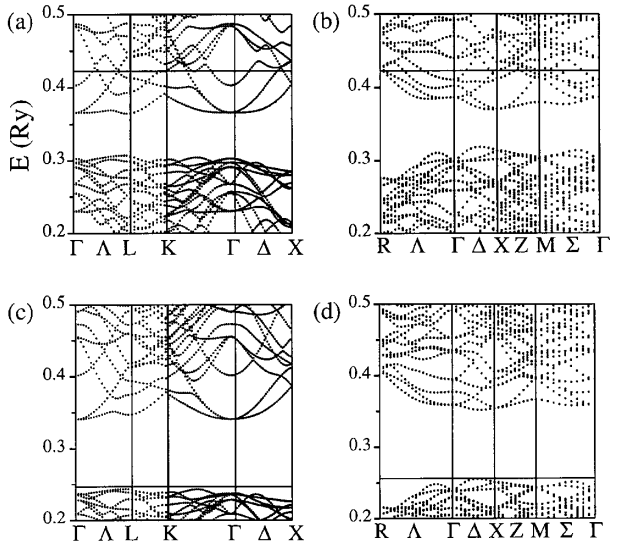

FIG. 2. Electronic band dispersion curves as obtained from FLAPW band structure calculations for (a) $Na_{24}Si_{136}$, (b) Na_8Si_{46}, (c) Si_{136}, and (d) Si_{46}.

Fundamental questions are how and why the clathrate structures are stabilized with respect to crystalline Si and the role of the Na dopant on the phase stability. In both elemental Si and the clathrates, each Si atom is bonded to four nearest neighbors. The difference between these structures is the way that these tetrahedra are packed and the dependence of the packing upon the valence electron concentration. The Si atoms in elemental Si are part of the six-member rings, whereas both five- and six-member rings are found in the clathrate structures [20]. Thus, it is important to understand the phase stability and its relationship to the structure. To explore this issue, the electronic structures are analyzed with the method of moments augmented with the second moment scaled tight-binding Hamiltonian [25]. This approach offers the advantage that one may decompose the results into structurally meaningful quantities in a much simpler way than in first principles methods and thus is ideal for a *qualitative* analysis of the dependence of phase stability upon electron concentration [25]. The ensuing discussion will assume complete charge transfer (*vide supra*) from Na and a rigid band model where only the Si atoms are considered. With this assumption the effective valence electron count for crystalline Si is $4e/\mathrm{Si}$ and for the type I Na_8Si_{46} it is $4.17e/\mathrm{Si}$, whereas for the type II Na_xSi_{136}, which exhibits a wide range of stoichiometries, it is between $4.0e/\mathrm{Si}$ ($x = 0$) and $4.18e/\mathrm{Si}$ ($x = 24$).

Figure 3(a) shows the total energy differences, obtained from tight-binding calculations [26], between the Si framework of the clathrates and that of elemental Si as a function of the number of valence electrons. The Si diamond lattice is most stable at effective electron counts from $4.0e/\mathrm{Si}$ to $4.4e/\mathrm{Si}$, while the next most stable structure is type II $Na_{24}Si_{136}$ then followed by the type I Na_8Si_{46} structure which becomes the most stable structure above $4.4e/\mathrm{Si}$. The shape of these energy difference curves can be fully understood in terms of the moments (μ_n) of the DOS. In general, the number of nodes (including the two end points) in these curves is equal to the moment which is most responsible for the energy difference between the two structures [25]. Within a tight-binding description these moments are theoretically connected to local structural features and thus may be used to relate the structural topology to the total electronic energy [25]. The energy difference curves can be reconstructed by expanding the DOS in terms of contributions from the various moments via a continued fraction expansion, which may be truncated at any given moment. It is clear from Fig. 3(a) that the energy difference curves between the clathrate structures and Si contain exactly five nodes indicating a strong μ_5 component which is related to the number of five-member rings which provide stability just above the half-filled band [25]. Since there are more five-member rings per Si in the $Na_{24}Si_{136}$ structure, it is more stable than Na_8Si_{46}. Thus the reconstructed DOS of Fig. 3(b) which contains only the energy components up to μ_5 is qualitatively correct

in terms of phase ordering. Inclusion of μ_6 [Fig. 3(c)], which is responsible for stabilizing elemental Si due to the large number of six-member rings in the diamond lattice, improves the agreement with the full calculation but does not qualitatively alter the trend.

This simple calculation captures the essence of the important trend that *both* clathrate structures are, in fact, only metastable with respect to disproportionation into Na and Si. The binding energies are estimated to be 0.1–0.2 eV above elemental Si, in agreement with more sophisticated calculations [10]. Furthermore, the predicted energetic ordering is also correct in that the $Na_{24}Si_{136}$ structure is only marginally more stable than Na_8Si_{46} [10]. However, the current analysis demonstrates that the clathrate structures are stabilized relative to Si at higher electron counts due to the formation of the five-member rings in these structures and should also be valid for other clathrate materials based on Ge or Sn. Thus the stability of the clathrates may be enhanced if the effective number of valence electrons on the clathrate framework could be increased.

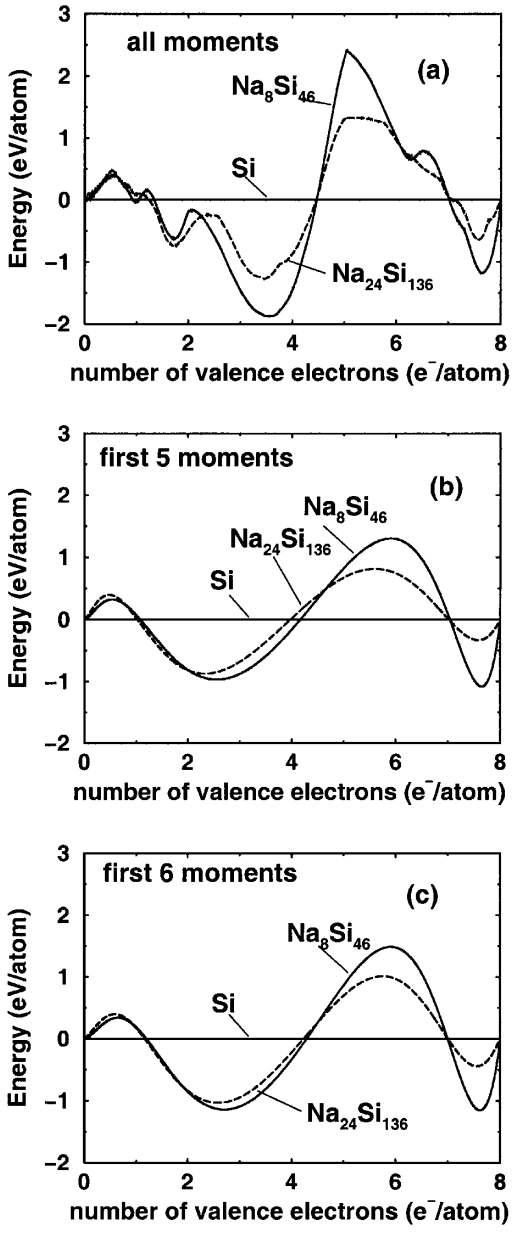

FIG. 3. Energy difference curves for elemental Si, type I Na_8Si_{46} and type II Na_8Si_{136}. The convention of these curves is that the structure with the highest energy is most stable at that electron count. (a) All moments, (b) up to 5th moment, and (c) including 6th moment.

It is essential to understand the dependence of the Seebeck coefficient on the Na dopant concentration. The Seebeck coefficient S can be computed from the knowledge of the Fermi surface of the conduction bands [27,28]. The results for the calculation on both type I and type II Na-doped Si clathrates are shown in Figs. 4(a) and 4(b), respectively. The calculations show that the larger the Na concentration the smaller the Seebeck coefficient. At low Na doping, such as Na_2Si_{46}, Na_6Si_{46}, and Na_8Si_{136}, the Seebeck coefficient has a large negative value that results from a delicate balance between electron and hole carriers. This trend is in good agreement with experiments [5,7,8] even though the calculated magnitudes are somewhat lower [29,30]. The calculated overall trend of S as a function of Na concentration may be ascribed to the band profile of the Si framework. Calculations performed on the Si_{46} clathrate, where the conduction bands are occupied simply by raising the Fermi level by an amount $\delta\varepsilon$, *qualitatively* reproduce the temperature dependence of S [Fig. 4(c)] and the important trend that lower concentrations of electropositive atoms lead to larger S. For low Na concentration only the lower energy conduction bands are occupied. These bands are sparse and relatively

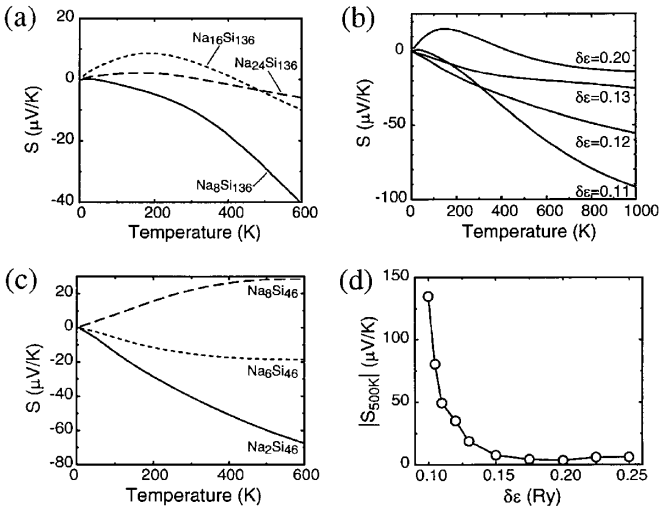

FIG. 4. Calculated Seebeck coefficient, S, for (c) Na_xSi_{46} ($x = 2$, 6, and 8) and for (a) Na_xSi_{136} ($x = 8$, 16, and 24). The Seebeck coefficient as obtained under a rigid band approximation for the compound Si_{46} (b). Here the effect of increasing dopant concentration is simulated by increasing the Fermi level above that found for the neutral cage by an amount $\delta\varepsilon$. The value of S as a function of $\delta\varepsilon$ at $T = 500$ K is shown in (d).

flat, resembling a semimetal. At higher Na concentration (i.e., higher Fermi level), the conduction bands are more free-electron-like resulting in a low Seebeck coefficient. Thus, lower concentrations of electron donating elements are desirable to maximize S.

Several general guidelines can be offered for the systematic improvement of the thermoelectric properties of clathrate based materials. Doping with more electrons may increase the stability of the clathrate phases, but it will result in lower values of the Seebeck coefficient. This difficulty can be circumvented by preparation with polyvalent electron releasing (electropositive) atoms, such as alkaline metals (group IIA) which donate more electrons and may be later extracted through distillation provided that the metal has sufficiently high vapor pressure [7,20]. In order to achieve efficient scattering of thermal phonons, the localized vibration frequencies of the dopant must not be higher than the maximum of the acoustic phonon branch of the framework. Clathrates with heavy dopant atoms and light framework elements will be desirable.

M. A. White thanks NSERC and the Killam Trusts for support.

[1] G. Mahan *et al.,* Phys. Today **50,** 42 (1997).
[2] A. A. Maradudin, Solid State Phys. **18,** 273 (1966).
[3] V. Narayanamurti and R. O. Pohl, Rev. Mod. Phys. **42,** 201 (1970).
[4] B. C. Sales *et al.,* Science **272,** 1325 (1996).
[5] G. S. Nolas *et al.,* Appl. Phys. Lett. **73,** 178 (1998).
[6] G. Slack *et al.,* Phys. Rev. Lett. **82,** 779 (1999).
[7] C. Cros *et al.,* J. Solid State Chem. **2,** 570 (1970).
[8] N. F. Mott, J. Solid State Chem. **6,** 348 (1973).
[9] H. Kawaji *et al.,* Phys. Rev. Lett. **74,** 1427 (1995).
[10] G. B. Adams *et al.,* Phys. Rev. B **49,** 8048 (1994); A. A. Demkov *et al., ibid.* **50,** 17 001 (1994).
[11] V. Smelyansky and J. S. Tse, Chem. Phys. Lett. **264,** 459 (1997). Note the degree of charge transfer from Na to the Si clathrate described in this work is at variance with the current study (see text). The discrepancy is due to incomplete analysis of the previous results and we retract these conclusions.
[12] D. Kahn and J. P. Lu, Phys. Rev. B **56,** 13 898 (1997); S. L. Fang *et al.,* Phys. Rev. B **57,** 7686 (1998).
[13] J. Dong *et al.,* Phys. Rev. B **60,** 950 (1999).
[14] J. S. Tse and M. A. White, J. Phys. Chem. **92,** 5006 (1988).
[15] J. S. Tse, J. Incl. Comp. Relat. Phenom. **17,** 259 (1994).
[16] J. S. Tse *et al.,* J. Chem. Phys. **107,** 9271 (1997).
[17] J. S. Tse *et al.* (to be published).
[18] V. V. Murashov and M. A. White, Rev. Sci. Instrum. **69,** 4198 (1998).
[19] L. Qui, M. A. White, and J. S. Tse (to be published).
[20] J. Kasper *et al.,* Science **150,** 1713 (1965).
[21] D. G. Cahill and R. O. Pohl, Annu. Rev. Phys. Chem. **39,** 93 (1988).
[22] P. Melinon *et al.,* Phys. Rev. B **59,** 10 099 (1999).
[23] First Principles FLAPW calculations were performed with program written by P. Blaha, K. Schwarz, and J. Luitz, WIEN97, improved and updated Unix version of the original copyrighted WIEN code which was published by P. Blaha *et al.,* Comput. Phys. Commun. **59,** 399 (1990). For SCF calculations, a 26–56 **k**-point mesh was used in the irreducible wedge of the Brillouin zone (BZ) to achieve convergence in the total energy of better than 0.0001 Ryd. The Fermi surfaces were generated with 20 000–40 000 **k**-point meshes using the interpolation scheme described in Ref. [28].
[24] J. Zhao *et al.,* Phys. Rev. B **60,** 14 177 (1999).
[25] S. Lee *et al.,* Phys. Rev. B **46,** 12 121 (1992); S. Lee, Annu. Rev. Phys. Chem. **47,** 397 (1996).
[26] For the tight-binding analysis, each Si atom is described by single exponent $3s$ and $3p$ Slater orbitals, the exponents of which were carefully chosen to match atomic wave functions as obtained from an atomic local density approximation calculation. A mesh of at least 1000 **k**-points over the symmetry-inequivalent portion of the BZ was used to ensure convergence of moments and energies.
[27] For crystals with a cubic structure, the Seebeck coefficient, $S(T)$, can be calculated from electronic relaxation time τ, density of states N, Fermi velocity ν, and Fermi distribution function f as
$$S(T) = I^1/eTI^0,$$
$$I^x = \int d\varepsilon\, \tau(\varepsilon, T)\,(\varepsilon - \varepsilon_F)^x N(\varepsilon)\nu^2(\varepsilon)[-\partial f(\varepsilon)/\partial\varepsilon]$$
[see J. M. Ziman, *Principles of the Theory of Solids* (Cambridge University Press, Cambridge, 1972), 2nd ed.]. To calculate the integrand at each energy point, Fermi surface integration is carried out using a dense k-point mesh, e.g., $34 \times 34 \times 34$ in the BZ. The relaxation time is eliminated in the expression for $S(T)$ if the isotropic approximation is employed.
[28] K. Uehara and J. S. Tse, Phys. Rev. B **61,** 1639 (2000).
[29] As noted in Ref. [9], even with well-compacted powder samples of apparently similar composition, the measured Seebeck coefficient can differ by a significant factor. We tested the computational procedure against a well characterized single crystal of β-Zn_4Sb_3. The calculated Seebeck coefficients were in very good agreement with experiment and also with a previous LAPW study [S. Kim *et al.,* Phys. Rev. B **57,** 6199 (1998)].
[30] N. P. Blake *et al.,* J. Chem. Phys. **111,** 3133 (1999).